

Neglecting the porosity of hot-star winds can lead to underestimating mass-loss rates

L. M. Oskinova, W.-R. Hamann, and A. Feldmeier

Lehrstuhl Astrophysik der Universität Potsdam, Am Neuen Palais 10, 14469 Potsdam, Germany
e-mail: lida@astro.physik.uni-potsdam.de

Received 11 September 2006 / Accepted 18 September 2007

ABSTRACT

Context. The mass-loss rate is a key parameter of massive stars. Adequate stellar atmosphere models are required for spectral analyses and mass-loss determinations. Present models can only account for the inhomogeneity of stellar winds in the approximation of small-scale structures that are optically thin. Compared to previous homogeneous models, this treatment of “microclumping” has led to reducing empirical mass-loss rates by factors of two to three. Further reductions are presently discussed in the literature, with far-reaching consequences e.g. for stellar evolution and stellar yields.

Aims. Stellar wind clumps can be optically thick in spectral lines. We investigate how this “macroclumping” influences the radiative transfer and the emergent line spectra and discuss its impact on empirical mass-loss rates.

Methods. The Potsdam Wolf-Rayet (PoWR) model atmosphere code is generalized in the “formal integral” to account for clumps that are not necessarily optically thin. The stellar wind is characterized by the filling factor of the dense clumps and by their average separation. An effective opacity is obtained by adopting a statistical distribution of clumps and applied in the radiative transfer.

Results. Optically thick clumps reduce the effective opacity. This has a pronounced effect on the emergent spectrum. Our modeling for the O-type supergiant ζ Puppis reveals that the optically thin $H\alpha$ line is not affected by wind porosity, but that the P V resonance doublet becomes significantly weaker when macroclumping is taken into account. The reported discrepancies between resonance-line and recombination-line diagnostics can be resolved entirely with the macroclumping modeling without downward revision of the mass-loss rate. In the case of Wolf-Rayet stars, we demonstrate for two representative models that stronger lines are typically reduced by a factor of two in intensity, while weak lines remain unchanged by porosity effects.

Conclusions. Mass-loss rates inferred from optically thin emission, such as the $H\alpha$ line in O stars, are not influenced by macroclumping. The strength of optically thick lines, however, is reduced because of the porosity effects. Therefore, neglecting the porosity in stellar wind modeling can lead to underestimating empirical mass-loss rates.

Key words. stars: mass-loss – stars: winds, outflows – stars: atmospheres – stars: early-type – stars: individual: ζ Puppis

1. Introduction

Mass loss by stellar winds plays a key role in the evolution of massive stars. The feedback of chemically enriched material, momentum, and mechanical energy is important for stellar clusters and the formation of stars, so it has consequences for the whole cosmic evolution (e.g. Leitherer et al. 1992; Woosley et al. 1993).

It is very important to know the mass-loss rate of stars in their different evolutionary phases, and its dependence on initial mass, composition, and possibly further parameters. Decades of efforts have been needed to establish reliable mass-loss rates for OB and Wolf-Rayet (WR) type stars (see Kudritzki & Puls 2000). Nevertheless, there are doubts whether the presently accepted mass-loss rates are correct. Some recent papers favor a dramatic downwards reduction of O-star mass-loss rates with far-reaching consequences. The reason for the uncertainties largely stem from the implications of wind inhomogeneity, i.e. “clumping”.

One of the numerous proofs of wind clumping is the line profile variability routinely found in O and WR spectra, where different types of variability can be distinguished. “Discrete absorption components” (DACs) are observed regularly in the UV spectra from O stars (e.g. Kaper et al. 1996). They display periodic patterns on timescales of days and are most likely associated with stellar rotation, but their slow wavelength drift is

still enigmatic (e.g. Hamann et al. 2001). “Modulations”, which have a slightly shorter timescale and are not strictly periodic, are thought to reflect non-radial stellar pulsations (Eversberg et al. 1998). Only the stochastic variability on short timescales of hours is attributed to wind clumping. Such stochastic variability has been studied by Lépine & Moffat (1999) in WR stars and by Markova et al. (2005) in the $H\alpha$ line of O stars.

Clear but indirect evidence for hydrodynamic shocks in O-star winds is the observed X-ray emission and the superionization that the X-rays produce in the cool plasma (Cassinelli & Olson 1979). Theoretical work has attributed such shocks to the intrinsic “de-shadowing” instability of line-radiation driven winds (Owocki et al. 1988; Feldmeier 1995).

A first approximation to account for clumping in stellar wind models has been introduced about a decade ago (Hamann & Koesterke 1998; Hillier & Miller 1999; Puls et al. 2006). It is based on the assumption that the wind clumps are small compared to the mean free path of the photons. This “microclumping” approximation introduces a new parameter D to describe the factor by which the density in the clumps is enhanced compared to a homogeneous model with the same mass-loss rate. The most important consequence of accounting for wind clumping within the optically-thin clump limit is the reduction of the empirical mass-loss rates by a factor \sqrt{D} . This holds in principle for all diagnostics that depend quadratically on the density,

thus including all emission lines in WR spectra, thermal radio emission, and the H α line from O stars. However, the different diagnostics may be affected to a different degree, due to the possible radial variation in the clumping factor D .

A handle for estimating the clumping factor in Wolf-Rayet atmospheres is provided by strong emission lines with extended line wings, caused by the frequency redistribution of line photons scattered by free electrons. Clumping reduces the relative strength of these wings, compared to homogeneous models (Hillier 1991), because typical WR emission lines scale with the square of density, while electron scattering scales linearly. Detailed modeling of electron scattering wings therefore allows the density enhancement factor D to be estimated.

Hamann & Koesterke (1998) typically found $D = 4$ for a few selected Galactic WN stars, corresponding to a volume filling factor of the clumps of $f_V = 0.25$. More recent studies (Crowther et al. 2002) prefer even stronger clumping, with filling factors smaller than $f_V = 0.1$.

For O-stars, Puls et al. (2006) conclude that the clumping factor D is about four times larger in the line-forming region, compared to the radio-emitting region far away from the star. Resonance lines, which are not affected by microclumping because of their linear density-dependence, are mostly saturated in O stars and therefore not suitable for precise mass-loss determinations. However, Fullerton et al. (2006) exploit the fact that the far-UV spectral range observed with FUSE contains the P V resonance line, which is typically unsaturated in O-star spectra, and analyze this line with the SEI method (1987). They derived mass-loss rates that are about ten times lower than obtained from ρ^2 diagnostics with unclumped models. Very strong clumping and consequently low mass-loss rates were also obtained by Bouret et al. (2005) for two O stars analyzed with non-LTE model atmospheres. Such low mass-loss rates would have dramatic consequences on stellar evolution and feedback.

However, all these downward-revisions of mass-loss rates are based on the assumption that the clumps are always smaller than the mean free path of photons. For strong lines in dense winds, this approximation cannot be justified. In the present paper we relax this small-clump approximation and account for clumps of arbitrary optical depth. Significant work has already been done to unveil the effects of optically thick inhomogeneities in stellar atmospheres.

Grey opacity in a stellar atmosphere where the photon mean free path does not exceed the scale of wind inhomogeneities was considered by Shaviv (1998). The term “porous atmosphere” was coined by Shaviv (2000) to describe a multi-phase medium that allows more radiation to escape while exerting a weaker average force. Such an atmosphere yields a considerably lower mass-loss rate for the same total luminosity and can explain the apparent existence of super-Eddington stars (Shaviv 2000). Owocki et al. (2004) introduced a “porosity-length” formalism to derive a simple scaling for the reduced effective opacity and used this to obtain an associated scaling for the continuum-driven mass-loss rate from stars that formally exceed the Eddington limit.

Continuum opacity in inhomogeneous winds with optically thick clumps was studied by Feldmeier et al. (2003). They considered X-ray lines emitted by an optically thin hot plasma that is attenuated in a fragmented cool stellar wind by strong continuum opacity from bound-free and K-shell photoionization processes. Oskinova et al. (2004) show that wind porosity can explain X-rays line profiles and the weak wavelength-dependence of the effective opacity. Considering the specific case of spherical clumps, Owocki & Cohen (2006) argue that a large clump

separation is required to fit the observed X-ray emission line profiles. However, Oskinova et al. (2006) reproduced the observed emission line profiles in X-ray spectra of O-stars with a wind model assuming plausible model parameters. Addressing mass-loss rates inferred from the analysis of radio measurements, Brown et al. (2004) point out that optically-thick clumping leads to the reduction of multiple scattering and, consequently, photon momentum delivery.

Line opacity in inhomogeneous stellar winds is modeled for the first time in the present paper. Considering the effect of clumping on UV resonance lines, Massa et al. (2003) and Fullerton et al. (2006) discuss how porosity can affect the formation of P Cygni lines and, in extreme cases, produce an apparently unsaturated profile for a line that would be extremely saturated if the wind material were distributed smoothly.

In the following section (Sect. 2) we briefly review the line radiative transfer in the conventional optically-thin clump approximation. In Sect. 3 we describe a statistical treatment for clumps of arbitrary optical thickness. In Sect. 4 both models are compared with observed mass-loss diagnostic lines in the spectrum of ζ Puppis. A brief parameter study is conducted in Sect. 5. Two representative examples of Wolf-Rayet model spectra are presented in Sect. 6, and a summary is given in Sect. 7.

2. Radiative transfer in the limit of optically thin clumps

Radiative transfer in an inhomogeneous medium is implemented in stellar-wind codes like CMFGEN and PoWR to a first approximation. This approximation holds in the limit that the size of the structures is small compared to the mean free path of photons (microclumping). Moreover, it is assumed that the inter-clump medium is void. The density in the clumps is enhanced by a factor of D compared to the density ρ of a smooth model with the same mass-loss rate \dot{M} ; hence, the volume filling factor is $f_V = D^{-1}$, where D may depend on the location in the stellar wind, i.e. on the radial coordinate r .

As there is no matter outside the clumps, rate equations are solved only for the clump medium, i.e. for the enhanced density $\rho_C = D\rho$. From the obtained population numbers, the non-LTE opacity and emissivity of the clump matter, $\kappa_C(D\rho)$ and $\eta_C(D\rho)$, can be calculated.

In the radiative transfer equation, the smooth-wind opacity and emissivity $\kappa(\rho)$ and $\eta(\rho)$ must be replaced for a clumped wind by

$$\kappa_f = f_V \kappa_C(D\rho) \quad \text{and} \quad \eta_f = f_V \eta_C(D\rho). \quad (1)$$

The factor f_V accounts for the fact that only this fraction of a ray actually crosses clumps. This treatment of radiative transfer is sometimes termed the “filling factor approach” (Hillier & Miller 1999).

The atomic processes contributing to the opacity and emissivity scale with different powers of the density. For processes *linear* in density, f_V and D cancel, but contributions scaling with the *square* of the density (bound-free emission, or free-free absorption and emission) are effectively enhanced by a factor of D . (Of course, κ and η are also indirectly affected by clumping via the population numbers, due to modified rates in the statistical equations.)

Empirical mass-loss diagnostics are widely based on processes that scale with the square of the density. The wind emission lines in Wolf-Rayet and O stars, including H α , form in de-excitation cascades that are fed by radiative recombination. The

thermal radio emission from stellar winds is due to the free-free process.

When the wind is clumped in the regions from which emission emerges, the radiation flux is enhanced by a factor of D compared to a homogeneous model with the same mass-loss rate. Consequently, when a given (radio or line) emission is analyzed with a model that accounts for microclumping, the derived mass-loss rate will be lower by a factor of \sqrt{D} than from with a smooth-wind model.

Puls et al. (2006) studied the O-type supergiant ζ Puppis and found that the mass-loss rates derived from H α and from IR/radio continuum emission can only be reconciled if the wind is strongly clumped ($D \approx 5.5$) already at a radius of $1.12 R_*$ where the wind velocity is only $\approx 100 \text{ km s}^{-1}$.

Line absorption coefficients depend linearly on density. In the case of resonance lines, the same holds for the re-emitted (“scattered”) photons. Hence, P Cygni profiles are independent of microclumping. Of course, clumping might indirectly affect resonance lines via the ionization balance. In most cases of practical importance, the resonance line belongs to the leading ionization stage, which is robust against such effects.

3. Radiative transfer with clumps of arbitrary optical thickness

The basic assumption of the “microclumping” approximation described in the previous section is that the clumps are small compared to the mean free path of photons, i.e. that they are optically thin. Given the large atomic opacity in the center of typical spectral lines, this approximation is not generally justified. In the present paper we therefore relax this approximation in favor of a more general treatment that accounts for the possibility of clumps being optically thick at some frequencies. We refer to this generalization as “macroclumping”.

3.1. Basic assumptions

To introduce our treatment of porous stellar winds, we first consider clumps that are smaller than the photon mean free path at any frequency. Throughout the paper, we refer to these as “microclumps”. The non-LTE population numbers that determine opacity and emissivity are obtained by solving the rate equations for the clump matter density. The radiation field that enters the radiative transition rates is calculated with these opacities and emissivities, corrected for the clump filling factor (cf. Eq. (1)).

As a next step, consider a few microclumps being merged together to form one bigger “macroclump” without changing the matter density. The size of this macroclump may now exceed the photon mean free path at frequencies with large atomic cross sections. In other words, the macroclump can be optically thick in the cores of a few strong spectral lines, while it remains optically thin at all other frequencies.

The non-LTE population numbers depend on the population and de-population processes, i.e. on the collisional and radiative transition rates. Because we assume that the clump density does not change by assembling the macroclump, collisional rates are not affected and are the same as calculated in the microclump approximation. The same holds for the radiative rates of optically thin transitions.

The only transition rates that change in the macroclump are those radiative rates that are excited at frequencies where the macroclump is optically thick. The radiation field in optically thick lines may change drastically in the inner parts of a clump.

However, in the optically thick limit, radiation is trapped inside the clump. Photons in these lines are immediately re-absorbed within the clump and do not escape to the interclump space.

The energy of photons in optically thick lines must be redistributed elsewhere: the population of the upper line level will increase until it is de-populated by other (radiative or collisional) transitions. Hence, in principle the radiation field in any other, optically thin line may be modified. We neglect this second-order effect and focus on the macroclumping effect on strong lines.

Photons in optically thick lines that emerge from the clump stem from its outer layers of optical depth about unity, irradiated from the interclump space. Therefore, even at these frequencies it is a reasonable approximation to adopt the radiation field from the microclumping model to evaluate the radiative transition rates, i.e. to neglect the feedback of macroclumping effects.

Summarizing these arguments, we find that

- (i) most of the transition rates are not affected at all by macroclumping (because they are collisional or excited by frequencies for which the clumps are optically thin), and
- (ii) for the few optically thick transitions, the average radiation field neglecting macroclumping provides a rough approximation to evaluate the radiative transition rates in the outer layers of the clumps.

Therefore it is a reasonable first approach to use the non-LTE population numbers from the microclumping model and to account for the macroclumping effects only in the “formal integral”.

3.2. Macro-clumping approach

For the radiative transfer in the “formal integral”, we use a statistical approach that holds within the limit of large clump number. As in the microclumping case, we assume that the density inside the clumps is enhanced by a factor of D compared to a smooth model with the same mass-loss rate. The interclump medium is void, and the volume filling factor is $f_V = D^{-1}$.

So far, no 3D simulations of stellar winds are available. Hydrodynamic 1D simulations of wind instabilities by Feldmeier et al. (1997) indicate that the clumps take the form of shell fragments. This is supported by detailed modeling of observed X-ray emission line profiles (Oskinova et al. 2006). On the other hand, Dessart & Owocki (2005) suggest that clumps may have a similar lateral and radial scale. However, they emphasize that the clump scale, compression level, and degree of anisotropy are still uncertain.

To avoid the introduction of an excessive number of free parameters, we assume here that clumps are isotropic. They have a linear size l that is uniform at a given distance from the stellar center but may be a function of radius r . For simplicity we assume that a clump of volume l^3 has diameter l for any crossing ray, thus neglecting any center-to-limb variation across the clump.

It is important to realize that we are considering *line* radiation transfer in a moving medium, which is transparent in the continuum. The situation is illustrated in Fig. 1. A specific ray, when crossing the stellar wind, only encounters line opacity over a short part of its path, where the projected expansion velocity has just the right value to Doppler-shift the line-center frequency to the selected observer’s frame frequency. In the framework of the Sobolev approximation, the observed line emission or absorption arises when the ray intersects the corresponding “constant radial velocity surface” (CRVS). In the case

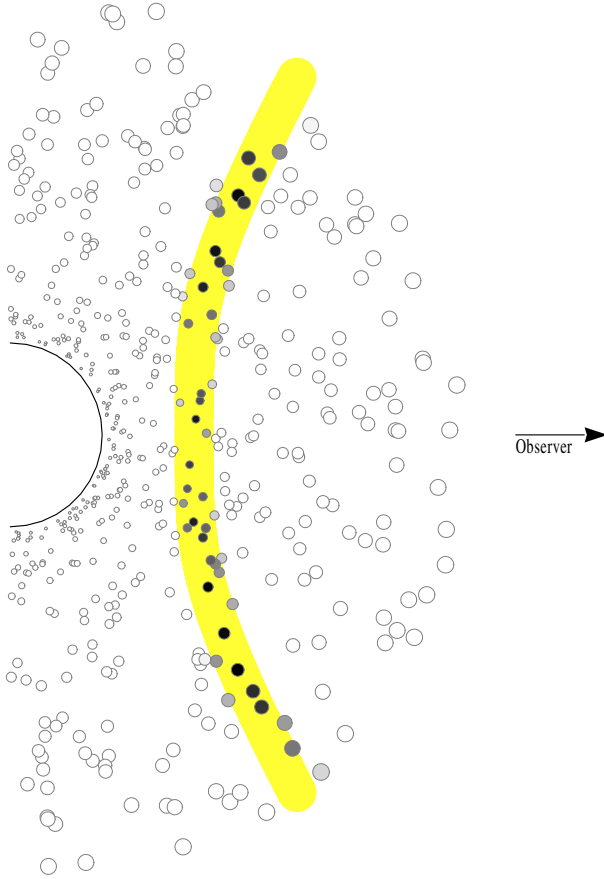


Fig. 1. Sketch of a clumped stellar wind. In a smooth wind, rays of a given observer’s frame frequency encounter line opacity only close to the “constant radial velocity surface” (CRVS, thick shaded line). In a clumpy wind, assuming that the clumps move with the same velocity law as in the homogeneous wind, only those clumps interact with the ray that lie close to the corresponding CRVS (dark-shaded circles). All other clumps are transparent (open circles) if the continuum opacity is small, so the wind is porous with respect to line absorption, even when the total volume is densely packed with clumps.

of a porous medium, the CRVS dissolves into patches. Adopting a clump/void density structure but an undisturbed velocity field, only those parts of the CRVS are effectively left that fall into the volume of a clump. Therefore, porosity effects can be especially important for *line* radiation transfer in expanding atmospheres.

We assume that the clumps are statistically distributed, having an average separation L between their centers ($L(r)$ varies with radial location); hence, the volume filling factor is $f_V = l^3/L^3$, or

$$D = L^3/l^3. \quad (2)$$

From Eq. (2) it follows that

$$n_C \equiv L^{-3} = D^{-1} l^{-3}, \quad (3)$$

where n_C denotes the number density of stochastically distributed clumps.

Lucy (2007) has shown that photospheric turbulence plays a decisive role in regulating the mass flux of a stationary flow. It is known from many studies that a high “microturbulence” is needed to reproduce the detailed shape of line profiles observed in O and WR star spectra. We identify this “microturbulence” v_D with the typical velocity dispersion within a clump,

caused by stochastic motions and the expansion of the clump itself. In our radiative transfer calculations, we therefore take the line absorption coefficient with a Gaussian profile corresponding to the Doppler-broadening velocity v_D and evaluate the optical depth across one clump formally as for a static medium.

We have already introduced the opacity κ_C *within* a clump, so we can write the optical depth across one clump with the help of Eq. (1) as

$$\tau_C = \kappa_C l = \kappa_f D l, \quad (4)$$

alternatively, τ_C can be expressed by the density contrast D and the average clump separation L ,

$$\tau_C = \kappa_f D^{2/3} L. \quad (5)$$

Note that for $L \rightarrow 0$ the clumps become optically thin, approaching the microclumping approximation.

The effective opacity κ_{eff} of the clumpy medium is obtained in analogy to the usual opacity from atomic absorbers:

$$\kappa_{\text{eff}} = n_C \sigma_C. \quad (6)$$

Here σ_C is the effective cross-section of a clump. “Effective” means that the geometrical cross section, l^2 , is multiplied by the fraction of photons that is absorbed when crossing the clump. As was derived in Feldmeier et al. (2003),

$$\sigma_C = l^2 (1 - e^{-\tau_C}). \quad (7)$$

Using Eq. (3) for the number of clumps and Eq. (7) for the effective cross-section in Eq. (6), the effective opacity becomes

$$\kappa_{\text{eff}} = (Dl)^{-1} (1 - e^{-\tau_C}). \quad (8)$$

In the limit of opaque clumps,

$$\lim_{\tau_C \rightarrow \infty} \kappa_{\text{eff}} = (Dl)^{-1}. \quad (9)$$

Noticing from Eq. (4) that $(Dl)^{-1} = \kappa_f/\tau_C$, we obtain a scaling of effective opacity with the opacity obtained in the microclumping approximation,

$$\kappa_{\text{eff}} = \kappa_f \frac{1 - e^{-\tau_C}}{\tau_C} \equiv \kappa_f C_{\text{macro}}. \quad (10)$$

The factor C_{macro} thus describes how macroclumping changes the opacity, compared to the microclumping limit. Note that the small-clump approximation $\kappa_{\text{eff}} \approx \kappa_f$ is recovered for optically thin clumps ($\tau_C \lesssim 1$). For optically thick clumps ($\tau_C \gtrsim 1$), however, the effective opacity is reduced by a factor C_{macro} compared to the microclumping approximation.

To understand the reduction of opacity in a medium with optically thick clumps, one can imagine that atomic absorbers are hidden in optically thick clumps and therefore not contributing to the effective opacity. Relatedly, Brown et al. (2004) noticed that this also leads to a reduction in radiative acceleration.

While Feldmeier et al. (2003) used Eqs. (6) and (7) for their analysis of X-ray emission line profiles, Eq. (10) was derived by Owocki et al. (2004) for the gray opacity. These authors define a “porosity length” $h \equiv L^3/l^2$. Rewriting Eq. (10) for the porosity length, one obtains $\kappa_{\text{eff}} = h^{-1} (1 - e^{-\tau_C})$. This can be compared to Eq. (A.7) in Feldmeier et al. (2003) and Eqs. (29) and (31) in Oskinova et al. (2004), where the opacity is allowed to be angular-dependent.

We evaluate the correction factor C_{macro} by specifying the clump separation $L(r)$, which enters Eq. (5) in combination with the density contrast $D(r)$. The reason for this parameterization is

that $D(r)$ must be specified for the density in the non-LTE rate equations. Note that the porosity length $h = D^{2/3}L$ alone is not adequate to define the model.

Clumps are assumed to be preserved entities. This assumption is corroborated by the hydrodynamical models (Feldmeier et al. 1997; Runacres & Owocki 2002; Dessart & Owocki 2005), that predict that the over-dense structures accelerate radially with $v(r)$ and, in general, do not split or merge. As a result, the number density of clumps has to obey the equation of continuity, $n_C \propto (r^2 v(r))^{-1}$.

Since the average clump separation is $L = n_C^{-1/3}$, we can write

$$L(r) = L_0 \left(r^2 w(r) \right)^{1/3}, \quad (12)$$

where L_0 is the free parameter of our macroclumping model. Note that r and L_0 are in units of the stellar radius, and $w(r) = v(r)/v_\infty$ is the velocity in units of the terminal speed.

Plausibly, L_0 is close to unity. In the 1D hydrodynamic model of Feldmeier et al. (1997), the wind shocks evolve from photospheric seed perturbations that have periods close to the acoustic cutoff. As the latter is close to the wind-flow time R_*/v_∞ for a typical O star, the predicted radial separation between the dense shells is approximately one stellar radius.

When studying the effect of macroclumping on the line spectra, it is important not to spoil the reference continuum. Therefore we only allow for macroscopic clumping in the line-forming regions, but suppress it in the photosphere. Photospheric clumping would alter the radiation field in the line-forming regions (and thus the population numbers!) and would also change (enhance) the reference continuum for the line spectrum.

Therefore we augment Eq. (12) for the clump separation L by a factor $s(\tau_{\text{Ross}})$, which switches the macroclumping off at large Rosseland optical depth, with a linear transition between τ_1 and τ_2 :

$$s(\tau_{\text{Ross}}) = \begin{cases} 0 & \text{if } \tau_{\text{Ross}} > \tau_2 \\ 1 & \text{if } \tau_{\text{Ross}} < \tau_1 \\ (\tau_2 - \tau_{\text{Ross}})/(\tau_2 - \tau_1) & \text{else} \end{cases} \quad (13)$$

where we usually choose $\tau_1 = 0.3$ and $\tau_2 = 1.0$. We have checked that the continuum flux (SED) is not modified by macroclumping effects with these parameters.

We implemented the described modifications of the radiative transfer into the “formal integral” of the PoWR model atmosphere code. At each integration step along each ray of given frequency, we calculated the clump optical depth τ_C from Eq. (5) and evaluated the macroclumping correction factor (Eq. (10)), which is applied to the opacity before the integration step is performed. Note that the same correction factor must also be applied to the emissivity to preserve the non-LTE source function according to our assumption that the population numbers are not affected.

3.3. Clump separation and the total number of clumps

The equations in the previous section describe our approach to optically thick clumping. Only one additional free parameter, L_0 , has been introduced compared to the microclumping approach (Eq. (12)). For a specified stellar atmosphere model, the choice of L_0 determines to what extend the clumps are optically thick at line frequencies. Within the limit of small L_0 , the macroclumping effects become negligible. Realistic values of L_0 can be estimated from considering the total number of clumps that reside in the wind at any given moment.

The number of clumps per unit volume, i.e. their number density, which is a statistical variable, follows from their average separation

$$n_C(r) = L^{-3} = \left(L_0^3 r^2 w(r) \right)^{-1}. \quad (14)$$

Thus the total number of clumps that are found within the radial range from r_1 to r_2 is

$$N_C = \int_{r_1}^{r_2} n_C(r) 4\pi r^2 dr = \frac{4\pi}{L_0^3} \int_{r_1}^{r_2} \frac{dr}{w(r)} = \frac{4\pi}{L_0^3} (t_2 - t_1), \quad (15)$$

where $t_2 - t_1$ is the flight time between r_1 and r_2 in units of the dynamical time scale, R_*/v_∞ . For “beta velocity laws” $v(r) = v_\infty(1 - 1/r)^\beta$, analytical solutions for certain values of β are given in Hamann et al. (2001). For $\beta = 1$ it holds that

$$t(r) = \int \frac{dr}{w(r)} = r + \ln(r - 1) + \text{const.} \quad (16)$$

Let us consider, for instance, the range between $r_1 = 1.05$, where the wind velocity is 5% of the terminal speed, and $r_2 = 10$ stellar radii. The total number of clumps in this volume obtained from the previous two equations is

$$N_C = 178 L_0^{-3}. \quad (17)$$

Note that N_C scales with r_2 more weakly than linearly; when restricting the volume to $r_2 = 5$, the number of enclosed clumps is still $N_C = 105 L_0^{-3}$.

Empirically, not much is known about the number of clumps in stellar winds. So far, only rough order-of-magnitude estimates can be made. Line profile variability may provide some relevant information. Lépine & Moffat (1999) monitored nine WR stars and found stochastic line profile variations in the form of narrow ($\approx 100 \text{ km s}^{-1}$) emission sub-peaks on top of emission lines. They explained their data by $10^3 \lesssim N_C \lesssim 10^4$ “blobs” being present at any time in the line emission region. Using Eq. (17) this corresponds to $L_0 \approx 0.3$. We will see in the next sections that a value of L_0 between 0.2 and 0.5, implying a plausible number of 10^3 to 10^4 clumps in the line-forming region, is high enough to produce significant macroclumping effects on the emergent spectra.

Further support for selecting L_0 in the range 0.1 to 1.0 comes from analyzing X-ray emission lines. In Oskinova et al. (2006), we reproduced the *Chandra* observations of O-star line profiles by assuming that spherical shells are ejected once per dynamic time scale $t_{\text{fl}} = R_*/v_\infty$, which corresponds to a radial separation of one stellar radius when v_∞ is reached. Note, however, that there are subtle differences between the “fragmented shell model” used for the X-ray modeling and the present paper, thereby preventing a direct comparison of the parameters.

4. The impact of macroclumping on O star spectra: ζ Puppis

As a representative test, we demonstrate the influence of macroclumping on the spectrum of the O-type supergiant ζ Puppis. First we calculate a non-LTE atmosphere model with the PoWR code (see Hamann et al. 2004, for details). Based on the model’s population numbers, the emergent spectrum is then obtained by solving the “formal integral”. This step is done twice, once with the usual code version that accounts for clumping only in the small-scale limit, and a second time with the macroclumping formalism as developed in the previous section.

For the macroclumping simulation, we set the clump separation parameter to $L_0 = 0.2$. According to Eq. (17), this implies a 2.2×10^4 clumps in the line-forming region (within $10 R_*$). This number of clumps is large enough to justify our statistical treatment, and it compares well with the empirical estimates (cf. Sect. 3.3).

Macroclumping is assumed to start at about the sonic point (10 km s^{-1}), together with microclumping. As model parameters for ζ Puppis, we adopt (compare Puls et al. 2006) $\log L/L_\odot = 5.9$, $T_* = 39 \text{ kK}$, $\log \dot{M}/(M_\odot \text{ yr}^{-1}) = -5.6$. We use the commonly accepted β -law for the velocity field, but split it into two ranges with $\beta = 0.9$ from the photosphere to $0.6 v_\infty$ and $\beta = 4$ for the outer part of the wind. The terminal speed v_∞ is 2250 km s^{-1} . The density enhancement factor is set to $D = 10$ in the supersonic part of the atmosphere. For the chemical composition, we adopt 42/56/0.12/0.4/0.9/0.14 (mass fractions in %) for the H/He/C/N/O/Fe-group (Repolust et al. 2004). We also included phosphorus with solar abundance (6.15×10^{-6} mass fraction).

We concentrate here on two lines, $H\alpha$ and the P V resonance doublet. The $H\alpha$ emission is the most important diagnostic tool for O-star mass-loss rates. The P V doublet, unlike other resonance lines, is not saturated (because of the low phosphorus abundance) and therefore potentially useful for the empirical determination of mass-loss rates. FUSE observations of the P V resonance doublet in the extreme ultraviolet caused the recent debate on a drastic downward revision of mass-loss rates (Fullerton et al. 2006; Bouret et al. 2005).

The $H\alpha$ emission line is strongly affected by microclumping, especially in the lower regions of the wind (see also Puls et al. 2006). In contrast to $H\alpha$, resonance lines are not sensitive to microclumping because of their linear dependence on density. Moreover, P V is the leading ionization stage of phosphorus in the wind of typical O stars. This makes the line robust against details of the modeling, including the “superionization” by X-rays, which is an essential effect for the O VI and N V resonance lines. For the same reason, the P V resonance doublet is also insensitive to the second-order effects on the population numbers that we neglect in our macroclumping approach, as discussed in Sect. 3.1.

Figure 2 displays the synthetic spectra from both model versions, without macroclumping use and with our macroclumping treatment, but otherwise identical parameters. The observation of ζ Pup is shown for comparison. The mass-loss rate of the model is tuned to the adopted density contrast $D = 10$ in order to obtain a good fit. We find that a model with the same mass-loss rate, but without microclumping, fails to reproduce the observed $H\alpha$ profile by far (the line appears in absorption).

Interestingly, the macroclumping effect is not significant for the $H\alpha$ line. We tested different L_0 and found no sensitivity for any realistic values. The obvious reason is that $H\alpha$ is optically thin in the supersonic part of the wind from ζ Pup, so accounting for macroclumping does not lead to a different empirical mass-loss rate from $H\alpha$ fitting.

When Bouret et al. (2005) and Fullerton et al. (2006) recently analyzed the P V resonance doublet in O-star spectra, they encountered severe discrepancies in the mass-loss rates inferred from $H\alpha$. They suggested that the only way to reconcile these different diagnostics is to assume much higher clumping contrast than assumed hitherto, implying a drastic reduction of the empirical mass-loss rates.

This discordance is illustrated in Fig. 3, showing the EUV spectrum of ζ Pup (from the COPERNICUS satellite) with the P V doublet. The continuous line is the synthetic spectrum of the conventional model without macroclumping. The parameters are

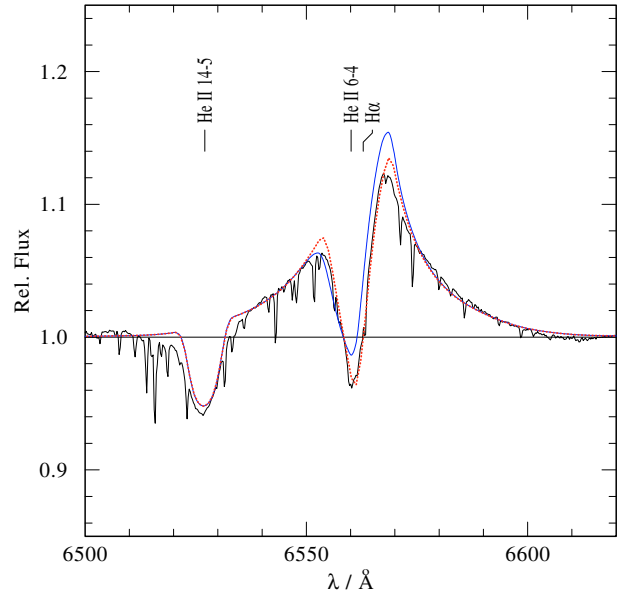


Fig. 2. Effect of macroclumping on the $H\alpha$ line from an O star. The observed spectrum of ζ Pup is shown for comparison (black, ragged line). The model parameters (see text) correspond to ζ Pup. The solid (blue) line results from a model that only accounts for small-scale clumping with a density contrast $D = 10$, switched on at the sonic point (10 km s^{-1}). The dotted (red) curve, partly identical with the solid (blue) curve, is obtained with macroclumping in the formal integral (also switched on at the sonic point with clump-separation parameter $L_0 = 0.2$). The effect of macroclumping on the $H\alpha$ emission is small.

the same as in Fig. 2, i.e. perfectly able to reproduce the observed $H\alpha$ emission. As can be seen, the predicted P-Cygni profiles of the P V doublet are much stronger than observed. To fit the $H\alpha$ and P V lines consistently with the microclumping model, a higher density contrast D and a lower mass-loss rate would be required.

Adopting the same model, we computed the stellar spectrum with our macroclumping formalism (Fig. 3). In the synthetic spectrum, the P V features are now drastically reduced, just to about the observed strength. Note that the numerous weak iron lines in this spectral range are not affected by the macroclumping correction. When accounting for macroclumping, the $H\alpha$ and P V lines in the observed spectrum of ζ Pup can be fitted simultaneously, using a “standard” clumping factor of $D = 10$ (filling factor $f_V = 0.1$). We conclude that accounting for macroclumping can result in a concordance of mass-loss estimates.

5. Influence of clump separation parameter, L_0 , and velocity dispersion within a clump, v_D

As explained in Sect. 3.2, L_0 is the essential free parameter of our macroclumping model. To demonstrate its influence, we consider the P V resonance doublet, keeping all other parameters as in the previous section. Blending iron lines are suppressed now for clarity.

We start by computing a model without macroclumping correction, i.e. $C_{\text{macro}} = 1$ implying $L_0 = 0$ from Eq. (5). The resulting profile is shown in Fig. 4. As the next step, we increase L_0 stepwise while all other parameters are kept constant. Increasing L_0 leads to an increased clump optical depth τ_C . Therefore, the macroclumping correction factor C_{macro} decreases, leading to a reduction of the effective opacity κ_{eff} . As can be seen in Fig. 4, higher values of L_0 result in weaker lines.

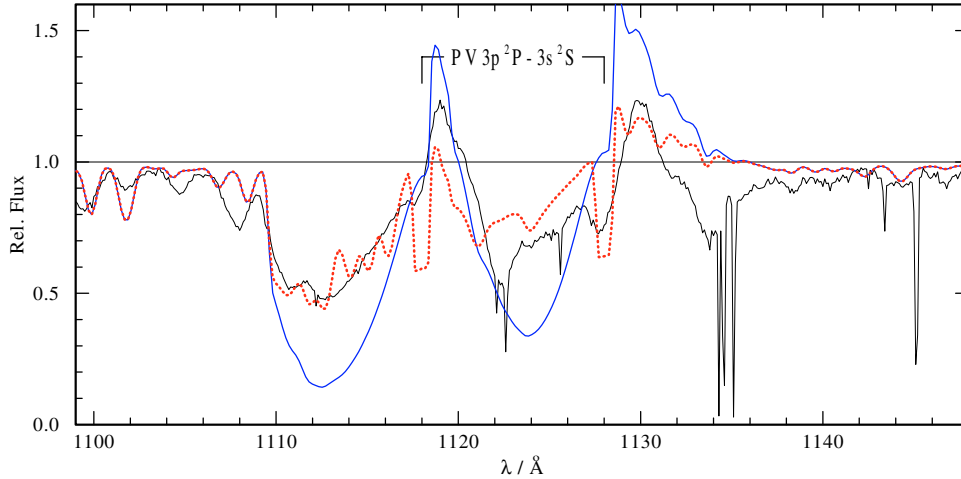


Fig. 3. Effect of macroclumping on the PV resonance doublet at 1118/1128 Å for an O star. The spectrum of ζ Pup as observed by COPERNICUS is shown for comparison (black, ragged line). The model parameters (see text) correspond to ζ Puppis. We adopt a microturbulence velocity of 50 km s^{-1} in the formal integral and do not apply rotational broadening; therefore the photospheric absorption components are not properly reproduced. Numerous weak spectral features in this range are due to iron. The usual microclumping modeling yields P Cygni features that are too strong (blue, continuous line). With our macroclumping formalism, the line features are reduced to the observed strength (red, dotted curve). Macro-clumping was switched on at about the sonic point (10 km s^{-1}) with a clump-separation parameter $L_0 = 0.2$.

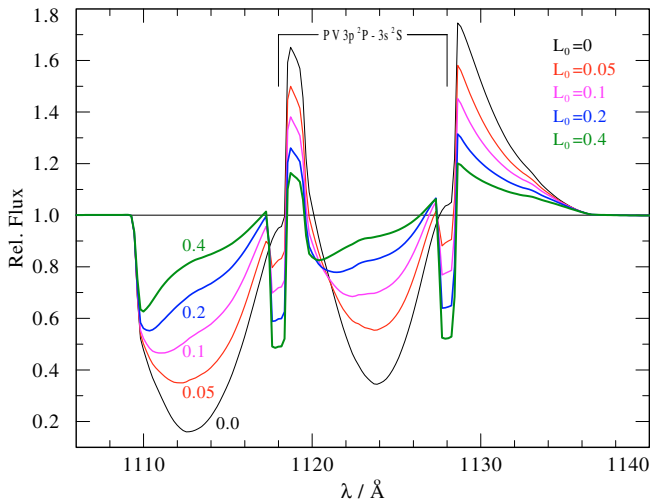


Fig. 4. Synthetic PV resonance doublet at 1118/1128 Å for different values of the clump separation parameter L_0 (labels). The model parameters are for ζ Pup (see Sect. 4), with $v_D = 50 \text{ km s}^{-1}$. A clump separation of zero recovers the microclumping limit. The larger the clump separation, the weaker the line becomes.

Significantly, the macroclumping effect depends not only on the number of clumps (defined by L_0), but also on the velocity dispersion within the individual clumps. This is a specific consequence of the line radiative transfer in an expanding wind. Figure 5 shows model lines that are computed with a constant parameter $L_0 = 0.2$, but for different velocities v_D . As can be seen, the porosity effect of reduced line strengths is stronger for lower values v_D .

To understand this result, we considered the line absorption coefficient in a clump. With lower velocity dispersion within a clump, the Doppler broadening is smaller, and the line absorption profile is narrower and peaks higher. Thus, the clump optical depth in the line core becomes larger, while it is smaller in the line wings. Higher optical depth in the line core leads to a reduction of the effective opacity and a weakening of the line (see Eq. (10)).

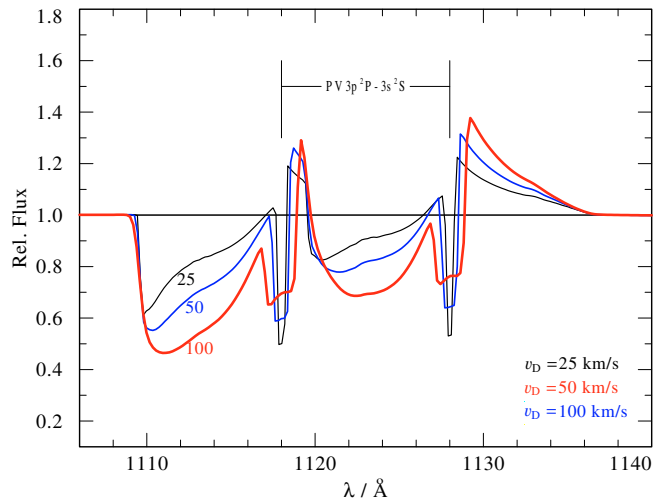


Fig. 5. Synthetic PV resonance doublet at 1118/1128 Å for different values of the microturbulence velocity v_D (labels). The clump separation parameter is $L_0 = 0.2$ for all cases. All other model parameters are kept fixed. When the velocity dispersion across the clumps is decreased, the macroclumping effect becomes more pronounced and leads to a weaker line profile. Note that the unrealistically strong photospheric absorption features become weaker with lower microturbulence velocities, as expected from the curve-of-growth effect.

This is in accordance with our interpretation of a porous constant velocity surface (see Sect. 3.2). As highlighted in Fig. 1, only clumps in the vicinity of the constant radial velocity surface contribute to the optical depth along the line-of-sight at a given frequency (see Sobolev 1947). In a wind with a monotonic velocity field $v(r)$, the characteristic width of this vicinity is given by the “Sobolev length”, $v_D/(dv/dr)$ (e.g. Grinin 2001). For lower Doppler-broadening velocity v_D , the clump is optically thick for a narrower range of frequencies within the line. Consequently the number of clumps that can contribute to the line-of-sight optical depth is smaller, and the effect of porosity is greater.

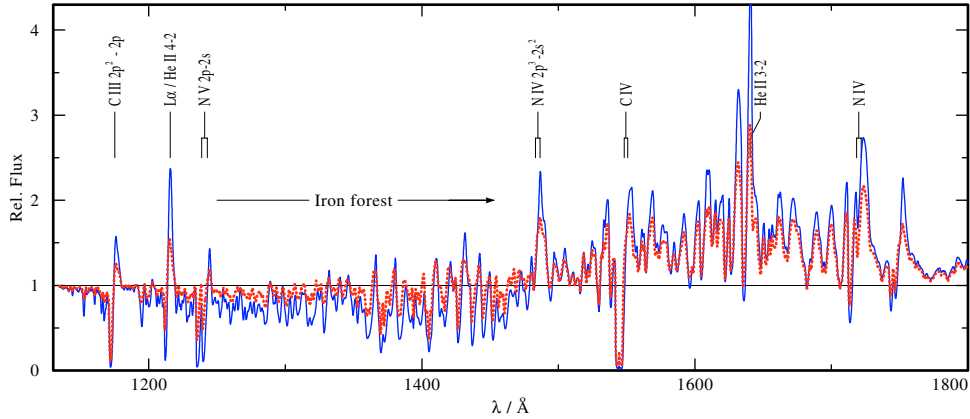


Fig. 6. Effect of macroclumping on the short-UV spectrum from a WN star of late subtype; the model parameters (see text) correspond to WR 78 (WN7h). The solid line is calculated with microclumping alone, and the dotted line is obtained with macroclumping in the formal integral (clump-separation parameter $L_0 = 0.5$).

The velocity dispersion across a clump is well-constrained both from empirical and theoretical considerations. It has been known for decades (e.g. Hamann 1980, Lamers et al. 1987) that detailed UV line fits for O stars require a “microturbulence velocity” of 50 to 100 km s⁻¹. The same holds for the emission line spectra of Wolf-Rayet stars. In our picture of a clumped wind, this small-scale Doppler broadening is identified with the typical velocity dispersion within one clump. Moreover, it has been noted repeatedly from monitoring line-profile variability that narrow features that appear transiently are never narrower than 50 to 100 km s⁻¹ (e.g. Lépine & Moffat 1999).

Clumps can only survive over the dynamic flow time when their internal velocity dispersion is small compared to the wind velocity, $v_D \ll v_\infty$. Close inspection of the 1D time-dependent model by Feldmeier et al. (1997) reveals that, within the density enhancements, the velocity does not differ by more than ≈ 100 km s⁻¹. Since v_D is constrained to 50 to 100 km s⁻¹ for O and WR stars, the clump separation L_0 is the basic free parameter of the macroclumping model.

6. Effect of macroclumping on Wolf-Rayet spectra

In this section we test the effect of macroclumping on the emergent spectra for representative models of a WNL star (i.e. a late-subtype Wolf-Rayet star of the nitrogen sequence), and a WNE (i.e. early-subtype Wolf-Rayet) star with strong emission lines.

The two examples are selected from the PoWR grid of models for WN stars. First we take a model with 20% hydrogen (“WNL grid” model WNL07-11, Hamann et al. 2004) with parameters corresponding to a late subtype (WN7): $T_* = 50$ kK, $\log R_t/R_\odot = 1.0$ (see Hamann et al. 2004 for the definition and role of this “transformed radius”). We use the standard β -law for the velocity field with $\beta = 1$ and $v_\infty = 1000$ km s⁻¹. The microturbulence velocity for Wolf-Rayet models is set to $v_D = 100$ km s⁻¹. In contrast to the published grid (www.astro.physik.uni-potsdam.de/~wrh/PoWR/powrgrid1.html), we choose here a density contrast of $D = 10$. The adopted composition is 78/20/1.5/0.01/0.14 for the mass fractions (in %) of the He/H/N/C/Fe-group. Except for the different (but scalable) luminosity, these parameters correspond to the Galactic Wolf-Rayet star WR 78. Compared to the previous example (ζ Pup), this model is slightly hotter and has a denser wind. In this example we have chosen a clump

separation parameter of $L_0 = 0.5$, i.e. the total number of clumps within $10 R_*$ according to Eq. (17) is 1424.

The UV spectrum (Fig. 6) shows numerous iron lines, partly in absorption and partly in emission at longer wavelengths. There are also a number of strong emission features, mostly as part of the P Cygni profiles. The highest emission peak is due to the He II 1640 Å transition. Comparing again the emergent spectrum with and without the macroclumping effect, we notice that generally all features, emission and absorption, are reduced in strength. Only the weakest lines are not affected, whereas the strongest emissions are cut down by more than 50%.

In the optical range similar reductions are found for strong lines, but Fig. 7 also demonstrates that the effect differs between individual lines of similar flux. Obviously, to restore a spectral fit with the macroclumping model, one would have to increase the mass-loss rate and possibly to re-adjust other parameters and abundances.

Our example with the densest wind corresponds to an early-subtype WN star with strong lines, WR 7 (WN4-s). The parameters are $\log L/L_\odot = 5.3$, $T_* = 112$ kK, $\log R_t/R_\odot = 0.3$, no hydrogen, $v_\infty = 1600$ km s⁻¹, $D = 10$. The chemical composition is the same as for the WNL model from Sect. 6, but without hydrogen. Except for the higher value of D , this model corresponds to the PoWR grid model WNE14-18 (Hamann et al. 2004). For the macroclumping correction, we again choose a clump separation of $L_0 = 0.5$.

The emergent spectra including macroclumping effects are shown in (Figs. 8 and 9). As expected, the macroclumping reduction is most pronounced for the strongest emission lines. As in the O star example, it is apparent that higher mass-loss rates must be chosen in order to maintain the lines as strong as they have been without macroclumping correction.

Interestingly, even the “iron forest” is now significantly affected by the porosity effect. This is because many of the iron lines in dense WR winds are quite strong (peak intensities up to four times the continuum, cf. Fig. 7), and form throughout the wind like any other lines of comparable strength.

Figure 10 demonstrates the influence of the clump separation parameter L_0 on the prominent He II emission line at 4686 Å. The emission decreases with increasing L_0 . This porosity effect is already significant for relatively small clump separation, like $L_0 = 0.1$.

In the process of a spectral analysis, one would have to compensate for this macroclumping effect by adopting a higher

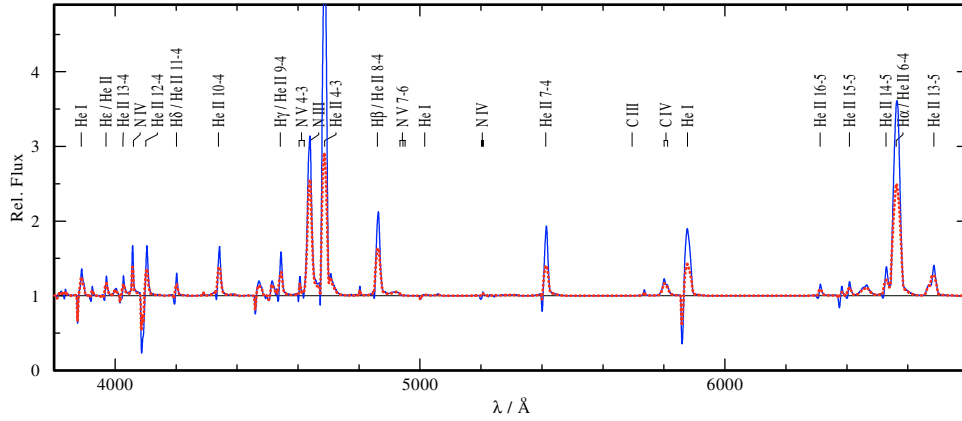


Fig. 7. Same as Fig. 6, but for the optical range.

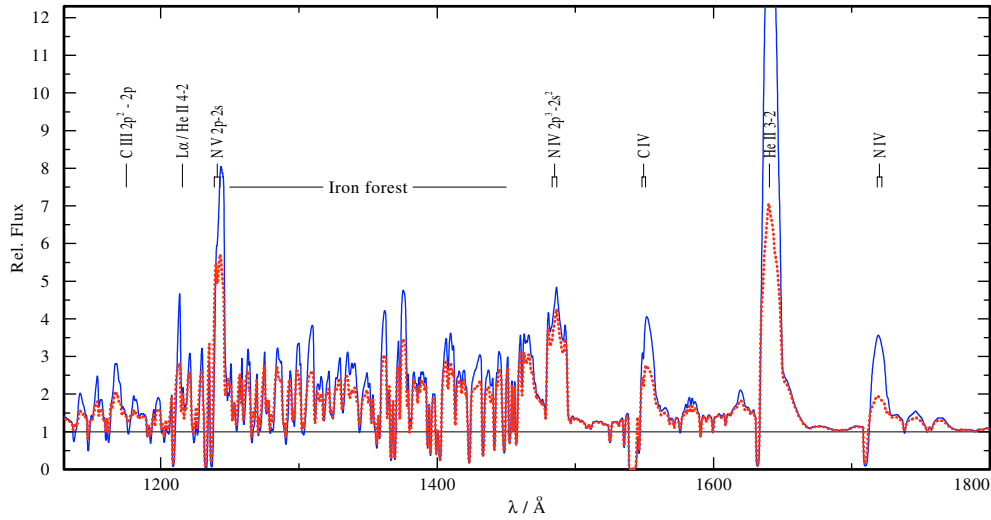


Fig. 8. Effect of macroclumping on the UV spectrum from a WN star of early subtype WR 7 (WN4-s) with parameters as given in the text. The solid line is calculated with microclumping alone, and the dotted line is obtained with macroclumping in the formal integral (clump-separation parameter $L_0 = 0.5$).

mass-loss rate. Changing \dot{M} , however, shifts the ionization balances. Given the different sensitivities of individual lines on the macroclumping effect (cf. Figs. 6–9), element abundances may become involved as well. It should also be noticed that the density contrast $D(r)$ may actually vary with radius. Thus it is by no means straightforward to achieve a new consistent spectral fit for WR stars with macroclumping, so we must leave this task for future work.

7. Summary

We have incorporated the effect of wind porosity into the “formal integral” of the PoWR non-LTE atmosphere code. In a statistical treatment, optically thick clumps lead to an effective reduction of the opacity. The feedback of macroclumping on the population numbers is neglected as a second-order effect, especially in the case of resonance lines from a leading ionization stage.

The effect of porosity on line formation differs drastically from that on the medium with continuous opacity. The effect of porosity on lines is enhanced due to the small extent of the zone where a ray is in resonance with the line frequency (“scattering zone”, “constant radial velocity surface”), while outside this zone the line opacity vanishes anyway due to the Doppler shift. Although a large number of clumps may be present in the wind,

only a limited number of these clumps contribute to the line opacity along a specific ray. The statistical treatment of porosity is corroborated by the time-averaging nature of observations. Even when the number of clumps that are present in the scattering zone at a given moment of time is small, there is a large number of clumps passing through this zone during a typical integration time of the observation.

Following the predictions of time-dependent hydrodynamic models, we assume that clumps are preserved entities and that there is no velocity gradient inside the clumps. The velocity dispersion within individual clumps is described by a “microturbulence” velocity that broadens the line opacity profile. For simplicity, the clumps are assumed to be isotropic.

We modeled the emergent spectrum of the O-type supergiant ζ Puppis and demonstrated the influence of macroclumping on the mass-loss diagnostic lines H α and P V. Whereas the optically thin H α line is not affected by wind porosity, the P V resonance doublet becomes significantly weaker when macroclumping is accounted for. Hence, neglecting macroclumping can lead to underestimating empirical mass-loss rates. In the case of ζ Pup, the discrepancy between the H α and P V diagnostic found by Fullerton et al. (2006) can be entirely resolved with the macroclumping modeling, without a downward revision of the mass-loss rate.

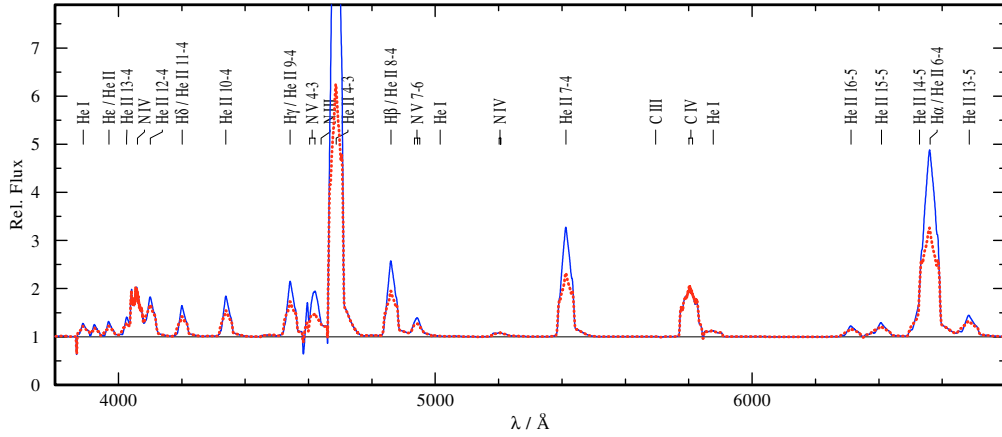


Fig. 9. Same as Fig. 8, but for the optical range.

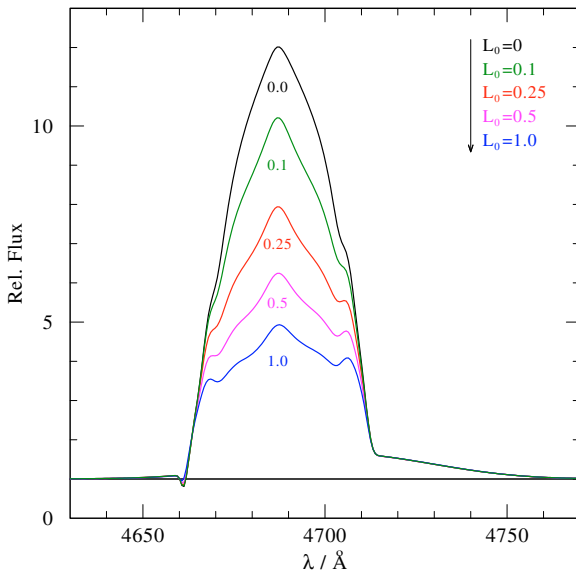


Fig. 10. Synthetic He II line at $\lambda 4686 \text{ \AA}$ in dependence on the clump separation parameter L_0 (see labels). $v_D = 50 \text{ km s}^{-1}$ for all lines. A clump separation of zero recovers the microclumping limit. The larger is the clump separation, the weaker the line becomes.

We also studied the influence of macroclumping on the emergent spectra for two representative Wolf-Rayet star models, corresponding to a WN star of late subtype and a WN star of early subtype with strong lines. The results show that basically all spectral features, in both emission and absorption, become significantly weaker when macroclumping is taken into account. Strong lines are typically reduced by a factor of two in intensity, while weak lines remain unchanged.

In spectral analysis, this weakening of lines must be compensated for by adopting a *higher* mass-loss rate. For emission lines that scale with ρ^2 because they are fed by recombination, macroclumping is counteracting microclumping in its effect on the empirical mass-loss rates.

Most important, wind porosity affects the P-Cygni profiles from resonance lines, in contrast to microclumping, which does not influence opacities that depend linearly on density. This can resolve the reported discrepancies between resonance-line and recombination-line diagnostics. Future work is needed to quantify this effect for individual stars.

Acknowledgements. This work has been supported by the Deutsche Forschungsgemeinschaft with grant Fe 573/3. The authors thank the referee for the thorough and thoughtful review that led to the significant improvement in the paper.

References

- Bouret, J.-C., Lanz, T., & Hillier, D. J. 2005, *A&A*, 438, 301
 Brown, J. C., Cassinelli, J. P., Li, Q., Kholtygin, A. F., & Ignace, R. 2004, *A&A*, 426, 323
 Cassinelli, J. P., & Olson, G. L. 1979, *ApJ*, 229, 304
 Crowther, P. A., Dessart, L., Hillier, D. J., Abbott, J. B., & Fullerton, A. W. 2002, *A&A*, 392, 653
 Dessart, L., & Owocki, S. P. 2005, *A&A*, 437, 657
 Eversberg, T., Lépine, S., & Moffat, A. F. J. 1998, *ApJ*, 494, 799
 Feldmeier, A. F. 1995, *A&A*, 299, 523
 Feldmeier, A., Kudritzki, R. P., Palsa, R., Pauldrach, A. W. A., & Puls, J. 1997, *A&A*, 320, 899
 Feldmeier, A., Oskinova, L. M., & Hamann, W.-R. 2003, *A&A*, 403, 217
 Fullerton, A. W., Massa, D. L., & Prinja, R. K. 2006, *ApJ*, 637, 1025
 Grinin, V. P. 2001, *Astrophysics* (English translation of *Astrofizika*), 44, 402
 Hamann, W.-R. 1980, *A&A*, 84, 342
 Hamann, W.-R., & Gräfener, G. 2004, *A&A*, 427, 697
 Hamann, W.-R., & Koesterke, L. 1998, *A&A*, 335, 1003
 Hamann, W.-R., Brown, J. C., Feldmeier, A., & Oskinova, L. M. 2001, *A&A*, 378, 946
 Hillier, D. J. 1991, *A&A*, 247, 455
 Hillier, D. J., & Miller, D. L. 1998, *ApJ*, 496, 407
 Hillier, D. J., & Miller, D. L. 1999, *ApJ*, 519, 354
 Kaper, L., Henrichs, H. F., Nichols, J. S., et al. 1996, *A&AS*, 116, 257
 Kudritzki, R.-P., & Puls, J. 2000, *ARA&A*, 38, 613
 Lamers, H. J. G. L. M., Cerruti-Sola, M., & Perinotto, M. 1987, *ApJ*, 314, 726
 Leitherer, C., Robert, C., & Drissen, L. 1992, *ApJ*, 401, 596
 Lépine, S., & Moffat, A. F. J. 1999, *ApJ*, 514, 909
 Lucy, L. B. 2007, *A&A*, 468, 649
 Markova, N., Puls, J., Scuderi, S., & Markov, H. 2005, *A&A*, 440, 1133
 Massa, D., Fullerton, A. W., Sonneborn, G., & Hutchings, J. B. 2003, *ApJ*, 586, 996
 Oskinova, L. M., Feldmeier, A., & Hamann, W.-R. 2004, *A&A*, 422, 675
 Oskinova, L. M., Feldmeier, A., & Hamann, W.-R. 2006, *MNRAS*, 372, 313
 Owocki, S. P., & Cohen, D. H. 2006, *ApJ*, 648, 565
 Owocki, S. P., Castor, J. I., & Rybicki, G. B. 1988, *ApJ* 335, 914
 Owocki, S. P., Gayley, K. G., & Shaviv, N. J. 2004, *ApJ*, 616, 525
 Puls, J., Markova, N., Scuderi, S., et al. 2006, *A&A*, 454, 625
 Repolust, T., Puls, J., & Herrero, A. 2004, *A&A*, 415, 349
 Runacres, M. C., & Owocki, S. P. 2002, *A&A*, 381, 1015
 Shaviv, N. J. 1998, *ApJ*, 494, 193
 Shaviv, N. J. 2000, *ApJ*, 532, 137
 Sobolev, V. V. 1947, *Moving Envelopes of Stars* [in Russian], Leningr. Gos. Univ., Leningrad (translated by S. Gaposchkin, Harvard Univ. Press, Cambridge, Mass., 1960)
 Woosley, S. E., Langer, N., & Weaver, Th. A. 1993, *ApJ*, 411, 823